

1 **Administration Routes for SSTR- / PSMA- and FAP-directed**
2 **Theranostic Radioligands in Mice**

3 Running title: Biodistribution of ⁶⁸Ga-ligands

4 Jasmin M. Klose¹, Jasmin Wosniack¹, Janette Iking¹, Magdalena Staniszewska¹, Fadi Zarrad¹,
5 Marija Trajkovic-Arsic^{2,3}, Ken Herrmann¹, Pedro Fragoso Costa¹, Katharina Lueckerath^{1,4},
6 Wolfgang P. Fendler¹

7 ¹ Department of Nuclear Medicine, University Hospital Essen, University of Duisburg-Essen,
8 Essen, Germany

9 ² Division of Solid Tumor Translational Oncology, German Cancer Consortium (DKTK), partner
10 site Essen, West German Cancer Center, University Hospital Essen, Essen, Germany

11 ³ German Cancer Consortium (DKTK) and German Cancer Research Center (DKFZ), Heidelberg,
12 Germany.

13 ⁴ Ahmanson Translational Theranostics Division, Department of Molecular & Medical
14 Pharmacology, David Geffen School of Medicine, University of California Los Angeles, USA.

15 Corresponding author:

16 Wolfgang Peter Fendler, M.D.

17 Address: Hufelandstraße 55, 45147 Essen, Germany

18 Telephone number: +49 201 723 2032

19 E-mail: Wolfgang.Fendler@uk-essen.de

20 First author:

21 Jasmin Mona Klose, PhD

22 Address: Hufelandstraße 55, 45147 Essen, Germany

23 Telephone number: +49 201 723 2032

24 E-mail: Jasmin.Klose@uk-essen.de

25 Word count: 4779

26 **ABSTRACT**

27 *Introduction:* The NETTER-1, VISION, and TheraP trials prove efficacy of repeat intravenous (i.v.)
28 application of small radioligands. Application by subcutaneous (s.c.), intraperitoneal (i.p.), or oral
29 (p.o.) access are important alternatives and may yield comparable or favorable organ and tumor
30 radioligand uptake. Here, we assess organ and tumor biodistribution for various radioligand
31 application routes in healthy mice and models of somatostatin receptor (SSTR)-, prostate-specific
32 membrane antigen (PSMA)-, and fibroblast activation protein (FAP)- expressing cancer.

33 *Methods:* Healthy and tumor-bearing male C57BL/6 or NOD SCID Gamma mice, respectively,
34 were applied with a mean of 6.0 ± 0.5 MBq ^{68}Ga -DOTATOC (RM1-SSTR allograft), 5.3 ± 0.3 MBq
35 ^{68}Ga -PSMA11 (RM1-PSMA allograft) or 4.8 ± 0.2 MBq ^{68}Ga -FAPI46 (HT1080-FAP xenograft) i.v.,
36 i.p., s.c. or p.o.. *In vivo* positron emission tomography and *ex vivo* biodistribution in tumor, organs,
37 and at the injection site were assessed up to 5h post injection (p.i.). Healthy mice were monitored
38 for up to 7 days after the last scan for signs of stress or adverse reactions.

39 *Results:* After i.v., i.p. and s.c. radioligand administration, average residual activity at the injection
40 site was $<17\%IA/g$ (1h p.i.), $<10\%IA/g$ (2h p.i.) and $\leq 4\%IA/g$ (4h p.i.) for all radioligands. Following
41 oral administration $\geq 50\%IA/g$ remained within the intestines until 4h p.i.. Biodistribution in organs
42 of healthy mice was nearly equivalent following i.v., i.p., and s.c. application at 1h p.i. and all
43 subsequent timepoints ($\leq 1\%IA/g$ for liver, blood and bone marrow; $11.2 \pm 1.4\%IA/g$ for kidneys). In
44 models for SSTR-, PSMA- and FAP-expressing cancer, tumor uptake was higher or equivalent for
45 i.p./s.c. versus i.v. injection at 5h p.i. (*ex vivo*): SSTR: $7.2 \pm 1.0\%IA/g$ ($p=0.0197$) / $6.5 \pm 1.3\%IA/g$
46 ($p=0.0827$) versus $2.9 \pm 0.3\%IA/g$; PSMA: $3.4 \pm 0.8\%IA/g$ ($p=0.9954$) / $3.9 \pm 0.8\%IA/g$ ($p=0.8343$)
47 versus $3.3 \pm 0.7\%IA/g$ and FAP: $1.1 \pm 0.1\%IA/g$ ($p=0.9805$) / $1.1 \pm 0.1\%IA/g$ ($p=0.7446$) versus
48 $1.0 \pm 0.2\%IA/g$.

49 *Conclusion:* In healthy mice, biodistribution of small theranostic ligands following i.p. or s.c.
50 application is nearly equivalent compared to i.v. injection. S.c. administration resulted in highest
51 absolute SSTR tumor and tumor-to-organ uptake as compared to the i.v. route, warranting further
52 clinical assessment.

53 **Keywords:**

54 radioligand, biodistribution, small animal PET, theranostic, intravenous, subcutaneous,
55 intraperitoneal, PSMA, SSTR, FAP, alternative application routes

56 INTRODUCTION

57 NETTER-1 (1), and the more recent clinical trials TheraP (2), and VISION (3), establish
58 somatostatin receptor (SSTR)- and prostate specific membrane antigen (PSMA)-directed small
59 ligand radiotheranostics as efficacious cancer therapy with favorable safety profiles. Recently,
60 fibroblast activation protein (FAP)-targeting small ligands have emerged for positron emission
61 tomography (PET) and therapy of cancers (4). Intravenous (i.v.) application is the standard route
62 for radioligand applications. However, oral (p.o.), intraperitoneal (i.p.), and subcutaneous (s.c.)
63 administrations are faster and require a lower level of training when compared to i.v., both in the
64 preclinical and clinical settings. The volume of preclinical and clinical radioligand applications is
65 growing rapidly and thus, there is an urgent unmet need to assess alternative application routes
66 to address the increasing demand. In addition, novel FAP-directed therapies are in a dynamic and
67 evolving process, highlighting the emerging need for an optimization of administration routes of
68 these novel radioligands for ongoing preclinical and clinical assessment. In this intent, assessment
69 of biodistribution and administration routes of ⁶⁸Ga-FAPI46 (fibroblast activation protein inhibitor)
70 was requested by the German Federal Institute for Drugs and Medical Devices (BfArM) for recent
71 approval of a prospective clinical trial on ⁶⁸Ga-FAPI46 PET/CT for various types of cancer
72 (NCT04571086).

73 We hypothesize that i.p. and s.c. application will yield near equivalent organ and tumor
74 biodistribution compared to the routine i.v. injection. We further hypothesized that organ and tumor
75 uptake will be significantly lower following p.o. application of radioligands. Here, we compare
76 tumor and organ biodistribution following i.v., i.p., s.c and p.o. application of small radioligands in
77 healthy mice and mouse models of SSTR-, PSMA-, and FAP-expressing cancer.

78

79 **METHODS**

80 **Cell Culture**

81 RM1 cells, virally stably transduced with SFG-Egfp/Luc (RM1-PGLS) or pMSCV-IRES-
82 YFP II-hSSTR (RM1-SSTR) to express high levels of cell surface human PSMA or SSTR2 (5),
83 were obtained from Johannes Czernin (University of California, Los Angeles). HT1080-FAP cells
84 were a gift from Uwe Haberkorn (University Hospital of Heidelberg). HT1080 cells were stably
85 transfected with the plasmid pcDNA1/neo-FAP (expressing the untagged full-length cDNA of
86 human FAP) followed by neomycin selection (6). RM1-PSMA and RM1-SSTR were maintained in
87 Roswell Park Memorial Institute 1640 medium (GIBCO) and HT1080-FAP in Dulbecco's Modified
88 Eagle Medium (GIBCO), both with 10% fetal bovine serum (Thermo Fisher Scientific) and 0.5%
89 penicillin/streptomycin (GIBCO), at 37°C with 5% CO₂. Cells were thawed 2 weeks or passaged
90 3 times before inoculation. Cells were routinely assessed for mycoplasma contamination using
91 the VenorGeM OneStep kit (Minerva Biolabs).

92 **Radiosynthesis**

93 ⁶⁸Ga-DOTATOC, ⁶⁸Ga-PSMA11 and ⁶⁸Ga-FAPI46 were obtained from the radiopharmacy
94 of our clinic. Clinical-grade radiolabeling of precursors (DOTATOC, PSMA11, FAPI46) was
95 performed using the Modular-Lab easy for DOTATOC and PSMA or Scintomics GRP 3V for FAPI
96 using commercially available reagent kits. The final solution had <5µg/mL for ⁶⁸Ga-DOTATOC,
97 <3µg/mL for ⁶⁸Ga-PSMA, and ~50µg/mL for ⁶⁸Ga-FAPI with 100µl injected volume per mouse.
98 Radiochemical purity was determined with radio-high-performance liquid chromatography. FAPI:
99 Chromolith Performance RP18e column from Merck (100 x 3mm) gradient: 0-20% MeCN+0.1%
100 TFA in 5 min run time 15 min; PSMA: 5-40% MeCN+0.1% TFA in 10 min run time 15 min;
101 DOTATOC: 24% MeCN+0.1% TFA for 8 min, then 24-60% in 1 min, run time 15 min; and thin-
102 layer chromatography (iTLC-SG, ammonium acetate (77g/L), methanol R (50:50 v/v)). The
103 radiochemical purity exceeded 98% for all radioligands.

104 **Mice and Tumor Models**

105 Male C57BL/6 and NOD SCID Gamma mice were purchased from Charles River
106 Laboratories (6-8 weeks old) and housed under specific pathogen-free conditions with food and

107 water available *ad libitum*. Health status monitoring of mice was performed by assessing a
108 summarized score twice a week (healthy animals) or daily (tumor-bearing animals). The study was
109 approved by the North Rhine-Westphalia State Agency for Nature, Environment and Consumer
110 Protection (LANUV), Germany (permit number: AZ.81-02.04.2018.A090).

111 For subcutaneous tumors, mice were injected with 0.1×10^6 RM1-SSTR cells or RM1-
112 PSMA (C57BL/6) or 1.0×10^6 HT1080-FAP (NOD SCID Gamma) in matrigel/PBS (50:50 ratio) into
113 the shoulder region. Tumor volume (V) was calculated by measuring the length (L) and width (W)
114 of tumors by caliper and using the formula $V = 1/2(L \times W^2)$ (7). PET scans were acquired 7-10
115 days after tumor inoculation, as described previously (5,8). Mean±SEM tumor volumes were
116 $0.39 \pm 0.09 \text{ cm}^3$ (interquartile range 0.07-0.66 cm^3) for RM1-SSTR tumors, $0.05 \pm 0.01 \text{ cm}^3$
117 (interquartile range 0.02-0.08 cm^3) for RM1-PSMA tumors, and $0.22 \pm 0.03 \text{ cm}^3$ (interquartile range
118 0.06-0.25 cm^3) for HT1080-FAP tumors.

119 Radioligand Application and Small Animal Positron Emission Tomography/Computed 120 Tomography (PET/CT)

121 Healthy or tumor-bearing anesthetized mice (1.5-2% isoflurane) received (mean±SEM)
122 $6.0 \pm 0.5 \text{ MBq}$ ^{68}Ga -DOTATOC, $5.3 \pm 0.3 \text{ MBq}$ ^{68}Ga -PSMA11 or $4.8 \pm 0.2 \text{ MBq}$ ^{68}Ga -FAPI46 i.v. (tail
123 vein), i.p., s.c. or p.o. (p.o. HT1080-FAP tumor-bearing mice only) (differences between injected
124 activities, $p = \text{n.s.}$). Each healthy mouse received i.v., i.p., s.c. and p.o. administration with 1 week
125 interval between PET/CT scans (Supplemental Figure 1A). Each tumor-bearing mouse was
126 scanned twice, at 1h and 4h p.i., following either i.v., i.p., or s.c. application and was sacrificed
127 ~5h p.i for *ex vivo* analysis (Supplemental Figure 1B). Imaging was performed with a β -CUBE
128 (PET) and X-CUBE (CT) (Molecubes) in temperature-controlled beds with monitoring of breathing
129 frequency. PET/CT was acquired (PET, 15 minutes; CT, 5 minutes) in list mode with frames for 5,
130 10 and 15 minutes (dynamic scans, maximum delay between injection and scan start 5 minutes)
131 and static scans 1h, 2h and 4h p.i. for healthy mice and 1h and 4h p.i. for tumor groups.

132 Image Reconstruction and Processing

133 Images were reconstructed using an iterative reconstruction algorithm (ISRA, 30 iterations)
134 with attenuation correction of the corresponding CT image. PET data were reconstructed into a
135 192×192 transverse matrix, producing a 400 μm isometric voxel size. PET images were evaluated
136 with PMOD software (PMOD Technologies LLC). Decay-corrected mean percent injected activity

137 per gram (%IA/g) of the tumor and organs of interest was derived from DICOM images. Volumes
138 of interest (VOIs) were defined as spheres of 5 mm (lung, liver, spleen, intestines, heart, brain,
139 kidneys) and 2.5 mm (bone marrow, thigh muscle, blood pool, injection site, tumor) diameter in
140 tissues of interest. %IA/g was calculated from the average pixel values reported in Bq/mL within
141 these VOIs corrected for radioactive decay and mouse body weight.

142 ***Ex Vivo* Analysis**

143 Approximately 5h p.i., animals were sacrificed and organs of interest were extracted,
144 dabbed dry, weighed, and radioactivity was measured in an automated gamma counter (Perkin-
145 Elmer Gamma Counter 2480 Wizard²). Organ and tumor uptake was calculated from radioactive
146 counts, decay-corrected and expressed as %IA/g.

147 **Data and Statistical Analysis**

148 Data are presented as mean±SEM unless indicated otherwise. All statistical analyses were
149 performed using GraphPad Prism (version 9.1.0; GraphPad Software). Tumor-to-organ uptake
150 ratios were calculated for blood, kidney, liver and bone marrow (femur) using %IA/g at 1h and 4h
151 in *in vivo* VOIs and at 5h for *ex vivo* gamma counter measurements (%IA/g tumor / %IA/g organ).
152 Statistical significance was assessed using Brown-Forsythe and Welch ANOVA test with
153 Dunnett's T3 multiple comparisons test or Tukey's multiple comparisons test. p-values below 0.05
154 were considered statistically significant. Statistically significant data are indicated by asterisks
155 (*p<0.05; **p<0.01; ***p<0.001; ****p<0.0001).

156 RESULTS

157 Local and Systemic Activity

158 To assess biodistribution of radioligands applied via different routes, we measured the
159 activity retained at the injection site versus the overall systemic activity distribution excluding the
160 application site. Activity at the injection site decreased over time following i.v., i.p. and s.c.
161 administration in healthy mice (Figure 1, Supplemental Figure 1). Residual activity at the injection
162 site 4h p.i. was (mean±SEM) for i.v.: $1.0\pm 0.3\%$ IA/g, i.p.: $4.4\pm 2.1\%$ IA/g and s.c.: $2.1\pm 0.5\%$ IA/g) for
163 all radioligands; this correlated inversely with increased systemic availability of radioligands. Oral
164 administration resulted in significant and prolonged retention of radioligands in the stomach and
165 proximal small bowel as well as a low systemic distribution (Figure 1A-C). Following p.o.
166 administration, average systemic uptake was highest for ^{68}Ga -FAPI46 (Figure 1C). Therefore, p.o.
167 application was further explored in HT1080-FAP tumor-bearing mice.

168 Near Equivalent Organ Biodistribution of Radioligands Following i.p., s.c., and i.v. 169 Application in Healthy Mice

170 In healthy mice, i.p., s.c., and i.v. injection of radioligands resulted in near equivalent organ
171 biodistribution *in vivo* (Figure 2-4, Supplemental Figures 2-3). Radioligand retention in blood and
172 kidney is listed in Supplemental Table 1. Blood retention in healthy mice was significantly higher
173 following i.p. or s.c. versus i.v. application of ^{68}Ga -PSMA11: i.p., 1h $p=0.0226$, 2h $p=0.0463$, and
174 4h $p=0.0394$; s.c., 1h $p=0.0880$, 2h $p=0.0021$, and 4h $p=0.065$. For ^{68}Ga -DOTATOC and ^{68}Ga -
175 FAPI46, blood and kidney distribution after i.p. and s.c. application were comparable to those
176 following i.v. injection (Figure 2-4). In further organs, including liver, bone marrow, lung, heart
177 spleen, intestines, brain and muscle, i.p., s.c., and i.v. application routes exhibited comparable
178 physiological biodistribution (Supplemental Figure 2). Moreover, in healthy mice, no short-term
179 and longer-term adverse effects of radioligand application and PET/CT procedures were noted
180 during the study duration (5 weeks).

181

182 **Increased or Comparable Tumor Uptake Following i.p. or s.c. Versus i.v. Injection of**
183 **Radioligands**

184 To evaluate the impact of the application route on tumor uptake of ^{68}Ga -DOTATOC, ^{68}Ga -
185 PSMA11, or ^{68}Ga -FAPI46, we assessed *in vivo* and *ex vivo* tumor and organ uptake in SSTR-,
186 PSMA- and FAP-expressing tumor models (Table 1, Figure 5-7, Supplemental Figures 4-5).

187 In mice bearing SSTR tumors, i.p./s.c. application resulted in significantly higher tumor
188 uptake (mean \pm SEM) when compared to i.v.: $p=0.0124$ / $p=0.0377$ at 1h; $p=0.0301$ / $p=0.0411$ at
189 4h; and $p=0.0197$ / $p=0.0827$ at 5h (*ex vivo*) (Table 1; Supplemental Figure 4). Tumor uptake of
190 ^{68}Ga -PSMA11 or ^{68}Ga -FAPI46 following i.p./s.c. injection of mice bearing PSMA- or
191 FAP-expressing tumors was comparable to the uptake observed after i.v. injection (Table 1).

192 Oral administration in mice bearing FAP-expressing tumors did not result in notable tumor
193 uptake (Table 1, Supplemental Figure 4). Oral application of ^{68}Ga -FAPI46 in tumor-bearing mice
194 yielded comparable biodistribution characteristics as seen in healthy mice (Supplemental Figure
195 4) with high gastrointestinal retention of the radioligand and low systemic distribution.

196 Tumor-to-organ uptake ratios of organs relevant for dosimetry (9, 10) for i.p./s.c. versus i.v.
197 application are depicted in Figure 5-7. I.p./s.c. application resulted in higher or equivalent tumor-
198 to-liver ratios at 5h p.i. when compared to i.v. (5h p.i. mean ratio \pm SEM): (i) ^{68}Ga -DOTATOC:
199 27.4 \pm 2.2-fold ($p=0.0138$) / 25.3 \pm 5.6-fold ($p=0.2756$) versus 13.9 \pm 2.9-fold; (ii) ^{68}Ga -PSMA11:
200 28.2 \pm 7.4-fold ($p=0.4504$) / 39.4 \pm 5.7-fold ($p=0.0259$) versus 16.9 \pm 2.8-fold; and (iii) ^{68}Ga -FAPI46:
201 6.1 \pm 1.6-fold ($p=0.4198$) / 12.0 \pm 1.1-fold ($p=0.0005$) versus 3.7 \pm 0.4-fold (Figure 5-7). Tumor-to-
202 bone marrow ratios were higher for i.p. compared with i.v. application in mice bearing SSTR-
203 expressing tumors: 50.7 \pm 4.3 versus 25.7 \pm 4.9 ($p=0.0096$) (Figure 5). S.c. application resulted in
204 higher tumor-to-blood ratios when compared with i.v. application in mice bearing PSMA-
205 expressing tumors: 24.5 \pm 4.2-fold versus 6.0 \pm 0.9-fold ($p=0.0186$). For other tumor-to-organ uptake
206 ratios no significant difference was observed (Figure 6). Oral application of ^{68}Ga -FAPI46 resulted
207 in negligible uptake in organs and tumors (Table 1, Supplemental Figure 4).

208 **DISCUSSION**

209 The current delivery method for radioligands for nuclear imaging or therapy is i.v. injection.
210 However, comparing different application routes is important for the translation of novel FAP
211 ligands and optimization of current clinical protocols for PSMA or SSTR ligands.

212 The current study aimed at comparing the biodistribution of SSTR-, PSMA-, and FAP-
213 directed small radioligands administered i.p., s.c., or p.o. with the standard i.v. application.
214 Alternative application routes may alter systemic distribution and tumor uptake (11-13), for
215 instance by slowing absorption due to a reduced rate of molecular transport via the lymphatics
216 and blood flow to the organs of interest/tumor (14).

217 Administration of small radioligands i.v., i.p., and s.c. was feasible and well tolerated as
218 assessed by a scoring system including behavior and overall physical appearance of mice. Small
219 radioligand systemic availability and biodistribution was comparable for i.p. and s.c. versus i.v.
220 application (Figure 1-4). In addition, i.p. and s.c. administration in mice resulted in significantly
221 higher ⁶⁸Ga-DOTATOC tumor uptake (Table 1), tumor-to-liver and tumor-to-bone marrow ratio in
222 SSTR-expressing tumors when compared with i.v. injection (Figure 5).

223 These findings have implications for preclinical and clinical radioligand administration,
224 since they could offer advantages for both fields. In mice, i.v. injection requires highly trained
225 personnel, and is more error-prone (e.g., paravenous injection) and time consuming. I.p. and s.c.
226 administration may serve as simple alternative application routes for imaging at later timepoints
227 after injection or therapy, allowing a higher throughput in mouse studies, with lower dropout rates
228 and high reproducibility. In mice, i.p. administration did not compromise radioligand tumor
229 accumulation despite a high initial absorbed dose in the intestines (15). However, due to slower
230 systemic bioavailability following i.p. or s.c. injection, i.v. application is recommended for early
231 dynamic imaging.

232 In clinical routine, usage of alternative application routes to i.v. may improve outpatient
233 care and benefit potential new therapy schemes allowing repeat radioligand application at short
234 interval.

235

236 In patients, i.p. application is limited due to a higher likelihood of infection or abdominal
237 organ damage. However, s.c. application is already well established as a standard route for
238 outpatient injectable medications and has an emerging role in delivery of biotherapeutics or
239 monoclonal antibodies (16,17). Indeed, in patients with accidental paravenous infusion of ¹⁷⁷Lu-
240 DOTATOC absorption from the paravenous injection site occurs with a half-life of less than 4h
241 (Supplemental Figure 6); this is in line with a short drainage observed following s.c. injection in
242 mice. We therefore expect that s.c. application in patients would be feasible.

243 Still, an increased radiation dose to organs such as kidneys, bone marrow, blood, lungs or
244 liver, may limit benefit from i.p./s.c. injection. However, if radioligand therapy regimens would be
245 changed to a weekly or biweekly schedule using s.c. application, activities for each administration
246 could probably be reduced in favor of these more frequent treatments. Weekly or biweekly i.p./s.c.
247 application could be realized by outpatient care, reducing the patient's time in hospital, personnel
248 capacities and thus, reduced costs.

249 In this study, the uptake in non-target tissues did not exceed critical values or radiation
250 dose as suggested from measured uptake in %IA/g (Figure 2-4). Therefore, we assume that a
251 detrimental radiation burden to organs at risk (mainly kidneys) after s.c. and i.p. application when
252 compared to the standard i.v. route is unlikely. Notably, preclinical and clinical studies for
253 DOTATOC- and PSMA-targeting radiotherapies demonstrated that after i.v. absorbed doses in
254 organs of risk are not likely to cause relevant radiotoxicity (9,10,18,19). However, to precisely
255 estimate the additional absorbed dose to the adjacent tissue (by i.p. and s.c.) following radioligand
256 therapy, further studies with Lu-177 labeled ligands and quantitative preclinical SPECT imaging
257 should be performed. Yet, if we assume a half-life of 2.3 hours for the change in local activity over
258 time at the injection site, as recently published by Tylski (20), we would not expect to detect a
259 change in dosimetry between one Lu-177 administration and, e.g., 2-3 administrations spaced by
260 48 h.

261 To date, the entire theranostics routine is based on rather conservative application
262 schemes with few possibilities of patient-specific modification. Our observation that s.c. application
263 showed similar tumor uptake as compared to i.v. may open up new opportunities for alternative
264 application schemes in the clinical routine – e.g., weekly or biweekly applications, which are less
265 feasible if using repeat i.v. injections. Also, s.c. application is faster and easier than i.v., and could
266 thus be realized in outpatient care by medical laboratory assistants in a time-efficient manner for
267 both, patient and clinic personnel. Furthermore, it would be interesting to investigate the influence
268 of i.v. application rate (applied dose per time) on tumor uptake. This could be realized in a clinical
269 study or observational trial on patients with poor vein status.

270 This study has some limitations. This study assessed ⁶⁸Ga-ligands for PET imaging and
271 did not examine therapeutic ¹⁷⁷Lu-labelled ligands. Furthermore, in-bed injection with concurrent
272 dynamic PET acquisition was not performed and due to the short ⁶⁸Ga half-life, timepoints beyond
273 5h p.i. were not feasible.

274 **CONCLUSION**

275 In mice, PET imaging after i.v., i.p., or s.c. injection of SSTR-, PSMA-, or FAP-directed
276 small radioligands is feasible. I.p. and s.c. administration of SSTR-ligands resulted in higher
277 absolute tumor and relative tumor-to-organ uptake compared to i.v., which may translate into
278 improved tumor irradiation in the setting of radioligand therapies and warrants further translational
279 assessment.

280 **DISCLOSURE**

281 WPF was a consultant for Janssen and Calyx, and he received fees from Bayer and
282 Parexel outside of the submitted work. KH reports personal fees from Bayer, personal fees and
283 other from Sofie Biosciences, personal fees from SIRTEX, non-financial support from ABX,
284 personal fees from Adacap, personal fees from Curium, personal fees from Endocyte, grants and
285 personal fees from BTG, personal fees from IPSEN, personal fees from Siemens Healthineers,
286 personal fees from GE Healthcare, personal fees from Amgen, personal fees from Novartis,
287 personal fees from ymabs, personal fees from Aktis Oncology, personal fees from Theragnostics,
288 personal fees from Pharma15, outside the submitted work. KL reports paid consulting activities
289 for Sofie Biosciences/iTheranostics, and funding from AMGEN outside of the submitted work. No
290 other potential conflict of interest relevant to this article was reported.

291 **ACKNOWLEDGMENTS**

292 We thank Prof. Dr. med Uwe Haberkorn for providing HT1080-hFAP cells, and the Nuclear
293 Medicine team at University Hospital Essen for their support. This study was funded in parts by
294 the Doktor Robert Pflieger-Stiftung, Hallstadt, Germany.

295

296 **KEY POINTS**

297 QUESTION: Are there alternatives to intravenous injection of SSTR-, PSMA-, or FAP-directed
298 radioligands?

299 PERTINENT FINDINGS: In healthy mice, i.p. and s.c. application of small radiotheranostic ligands
300 resulted in near equivalent systemic availability and organ biodistribution at early (1h) and late
301 (4h) timepoints p.i. when compared to i.v. injection. I.p./s.c. administration significantly increased
302 absolute tumor and relative tumor-to-organ uptake in SSTR tumors (⁶⁸Ga-DOTATOC) compared
303 to i.v. route.

304 IMPLICATIONS FOR PATIENT CARE: I.p. and s.c. application is feasible in animal models of
305 small radioligand imaging or therapy. Tumor uptake and tolerability of s.c. application warrants
306 assessment in clinical studies.

307

308 **REFERENCES**

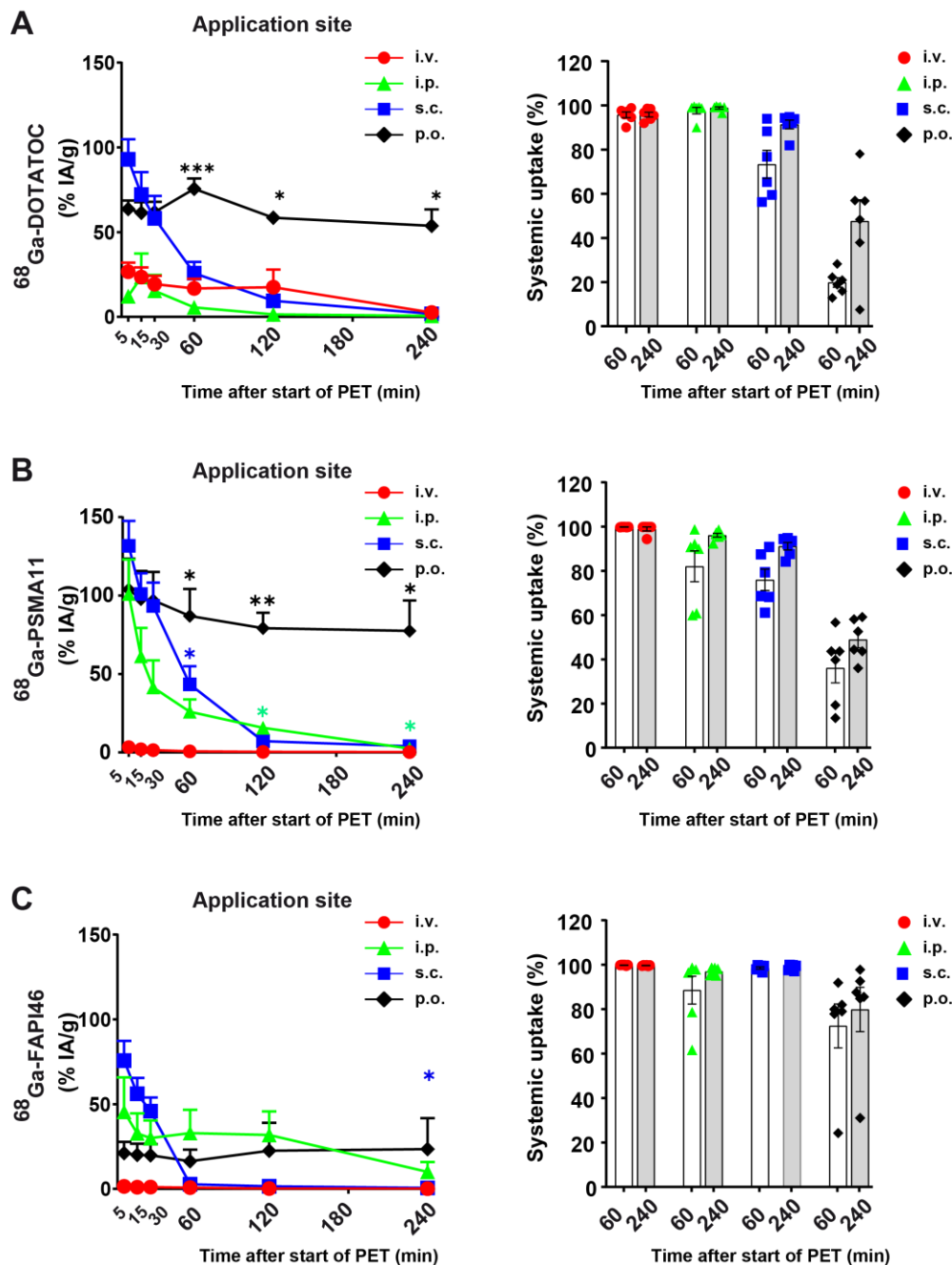
- 309 1. Strosberg J, Wolin E, Chasen B, et al. NETTER-1 phase III in patients with midgut
310 neuroendocrine tumors treated with 177Lu-Dotatate: Efficacy and safety results. *J Nucl Med.*
311 2016;57:629-629.
- 312
313 2. Hofman MS, Emmett L, Sandhu S, et al. [(177)Lu]Lu-PSMA-617 versus cabazitaxel in
314 patients with metastatic castration-resistant prostate cancer (TheraP): a randomised, open-
315 label, phase 2 trial. *Lancet.* 2021;397:797-804.
- 316
317 3. Sartor O, de Bono J, Chi KN, et al. Lutetium-177-PSMA-617 for metastatic castration-resistant
318 prostate cancer. *N Engl J Med.* 2021;385(12):1091-1103.
- 319
320 4. Hathi DK, Jones EF. (68)Ga FAPI PET/CT: Tracer uptake in 28 different kinds of cancer.
321 *Radiol Imaging Cancer.* 2019;1:e194003.
- 322
323 5. Fendler WP, Stuparu AD, Evans-Axelsson S, et al. Establishing (177)Lu-PSMA-617
324 radioligand therapy in a syngeneic model of murine prostate cancer. *J Nucl Med.*
325 2017;58:1786-1792.
- 326
327 6. Loktev A, Lindner T, Burger EM, et al. Development of fibroblast activation protein-targeted
328 radiotracers with improved tumor retention. *J Nucl Med.* 2019;60:1421-1429.
- 329
330 7. Jensen MM, Jorgensen JT, Binderup T, Kjaer A. Tumor volume in subcutaneous mouse
331 xenografts measured by microCT is more accurate and reproducible than determined by 18F-
332 FDG-microPET or external caliper. *BMC Med Imaging.* 2008;8:16.
- 333
334 8. Luckerath K, Stuparu AD, Wei L, et al. Detection threshold and reproducibility of (68)Ga-
335 PSMA11 PET/CT in a mouse model of prostate cancer. *J Nucl Med.* 2018;59:1392-1397.
- 336
337 9. Sandstrom M, Garske-Roman U, Granberg D, et al. Individualized dosimetry of kidney and
338 bone marrow in patients undergoing 177Lu-DOTA-octreotate treatment. *J Nucl Med.*
339 2013;54:33-41.
- 340
341 10. Delker A, Fendler WP, Kratochwil C, et al. Dosimetry for (177)Lu-DKFZ-PSMA-617: a new
342 radiopharmaceutical for the treatment of metastatic prostate cancer. *Eur J Nucl Med Mol*
343 *Imaging.* 2016;43:42-51.
- 344
345 11. Strigari L, Konijnenberg M, Chiesa C, et al. The evidence base for the use of internal
346 dosimetry in the clinical practice of molecular radiotherapy. *Eur J Nucl Med Mol Imaging.*
347 2014;41:1976-1988.
- 348
349 12. Gafita A, Rauscher I, Retz M, et al. Early experience of rechallenge (177)Lu-PSMA
350 radioligand therapy after an initial good response in patients with advanced prostate cancer.
351 *J Nucl Med.* 2019;60:644-648.

- 352
353
354
355
13. Current K, Meyer C, Magyar CE, et al. Investigating PSMA-targeted radioligand Therapy efficacy as a function of cellular PSMA levels and intratumoral PSMA heterogeneity. *Clin Cancer Res.* 2020;26:2946-2955.
- 356
357
358
359
14. Sanchez-Felix M, Burke M, Chen HH, Patterson C, Mittal S. Predicting bioavailability of monoclonal antibodies after subcutaneous administration: Open innovation challenge. *Adv Drug Deliv Rev.* 2020;167:66-77.
- 360
361
362
363
15. Dou S, Smith M, Wang Y, Rusckowski M, Liu G. Intraperitoneal injection is not always a suitable alternative to intravenous injection for radiotherapy. *Cancer Biother Radiopharm.* 2013;28:335-342.
- 364
365
366
16. Bittner B, Richter W, Schmidt J. Subcutaneous administration of biotherapeutics: An overview of current challenges and opportunities. *BioDrugs.* 2018;32:425-440.
- 367
368
369
17. Viola M, Sequeira J, Seica R, et al. Subcutaneous delivery of monoclonal antibodies: How do we get there? *J Control Release.* 2018;286:301-314.
- 370
371
372
373
18. Wehrmann C, Senftleben S, Zachert C, Muller D, Baum RP. Results of individual patient dosimetry in peptide receptor radionuclide therapy with ¹⁷⁷Lu DOTA-TATE and ¹⁷⁷Lu DOTA-NOC. *Cancer Biother Radiopharm.* 2007;22:406-416.
- 374
375
376
377
378
19. Kabasakal L, AbuQbeitah M, Aygun A, et al. Pre-therapeutic dosimetry of normal organs and tissues of (¹⁷⁷)Lu-PSMA-617 prostate-specific membrane antigen (PSMA) inhibitor in patients with castration-resistant prostate cancer. *Eur J Nucl Med Mol Imaging.* 2015;42:1976-1983.
- 379
380
381
20. Tylski P, Pina-Jomir G, Bournaud-Salinas C, Jalade P. Tissue dose estimation after extravasation of (¹⁷⁷)Lu-DOTATATE. *EJNMMI Phys.* 2021;8:33.
- 382
383

Tables

385 **Table 1. I.p. or s.c. application led to higher or equivalent tumor uptake compared to i.v**
 386 **injection.** Mice with subcutaneous RM1-SSTR, RM1-PSMA or HT1080-FAP tumors were injected
 387 with ⁶⁸Ga-DOTATOC, ⁶⁸Ga-PSMA11 or ⁶⁸Ga-FAPI46. Absolute tumor uptake (%IA/g) at 1h and
 388 4h p.i. (*in vivo* PET), and 5h p.i. (*ex vivo* gamma counter) is given. Data are represented as mean
 389 %IA/g±SEM of *n*=6 mice/group. **p*<0.05; ***p*<0.01.

RM1-SSTR (⁶⁸ Ga-DOTATOC)							
	i.v.	i.p.	s.c.	p-value i.v. vs. i.p.	p-value i.v. vs. s.c.		
<i>in vivo</i> 1 h	5.3 ± 0.6	9.9 ± 1.0	10.8 ± 1.6	p=0.0124*	p=0.0377*		
<i>in vivo</i> 4 h	4.4 ± 0.7	8.6 ± 1.1	11.1 ± 2.0	p=0.0301*	p=0.0411*		
<i>ex vivo</i> 5 h	2.9 ± 0.3	7.2 ± 1.1	6.5 ± 1.3	p=0.0197*	p=0.0827		
RM1-PSMA (⁶⁸ Ga-PSMA11)							
	i.v.	i.p.	s.c.	p-value i.v. vs. i.p.	p-value i.v. vs. s.c.		
<i>in vivo</i> 1 h	2.9 ± 0.2	3.0 ± 0.6	2.6 ± 0.4	p=0.9837	p=0.8297		
<i>in vivo</i> 4 h	2.6 ± 0.2	2.6 ± 0.7	2.9 ± 0.5	p=0.9996	p=0.8289		
<i>ex vivo</i> 5 h	3.3 ± 0.7	3.4 ± 0.8	3.9 ± 0.8	p=0.9954	p=0.8343		
HT1080-FAP (⁶⁸ Ga-FAPI46)							
	i.v.	i.p.	s.c.	p.o.	p-value i.v. vs. s.c	p-value i.v. vs. s.c	p-value i.v. vs. p.o.
<i>in vivo</i> 1 h	1.2 ± 0.2	2.0 ± 0.4	2.2 ± 1.1	0.1±0.03	p=0.3024	p=0.6732	p=0.0032**
<i>in vivo</i> 4 h	1.0 ± 0.2	1.5 ± 0.3	1.1 ± 0.6	0.1±0.04	p=0.4559	p=0.9911	p=0.0087**
<i>ex vivo</i> 5 h	1.0 ± 0.2	1.1 ± 0.1	1.4 ± 0.4	0.02±0.01	p=0.9805	p=0.7446	p=0.0058**

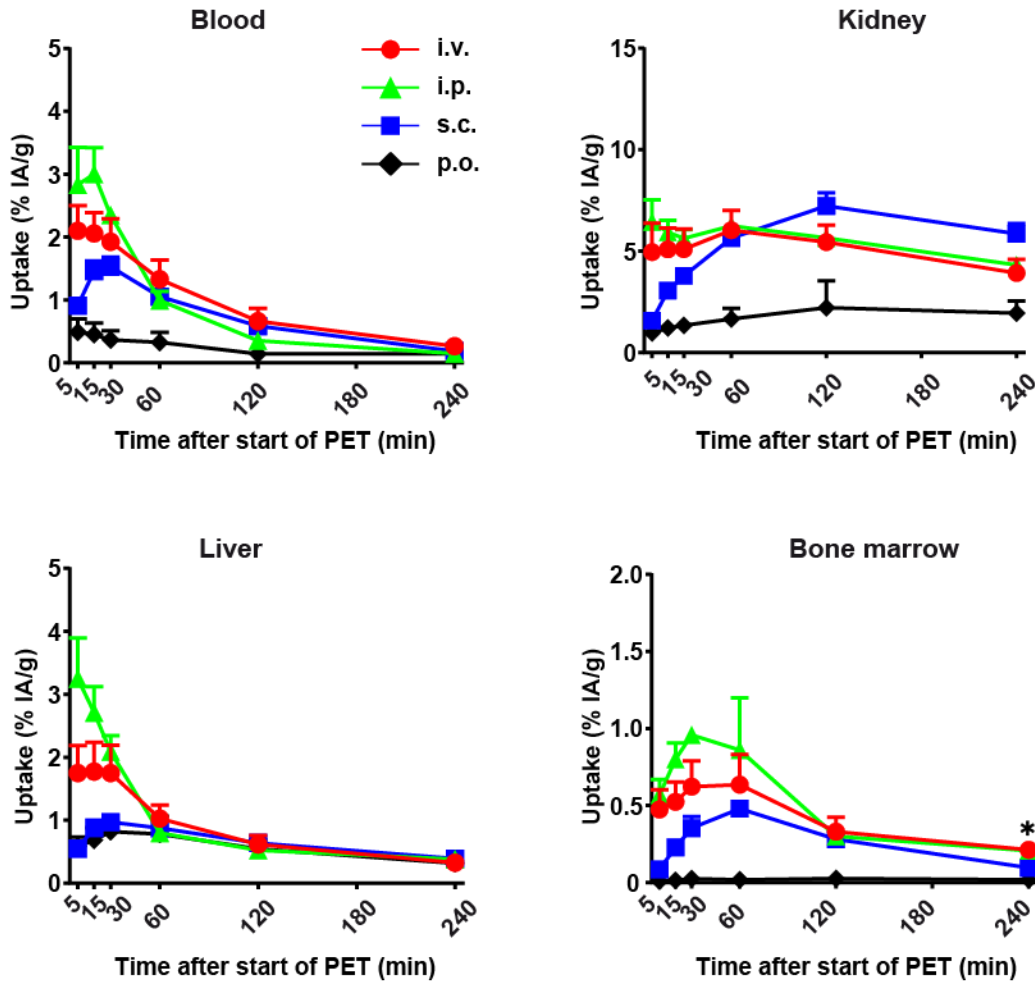


390
391

392 **Figure 1. Activity at the application site and systemic availability over time in healthy mice.**

393 Retention of (A) ^{68}Ga -DOTATOC, (B) ^{68}Ga -PSMA11, and (C) ^{68}Ga -FAPI46 in healthy mice
 394 ($n=6/\text{group}$) at the application site. *Left panel:* Time activity curves illustrate radioligand dynamics
 395 at the application site for i.v., i.p., s.c., and p.o. application. *Right panel:* Relative systemic uptake
 396 of whole body VOI excluding application site VOI displayed in % of total body uptake. Each dot
 397 represents a mouse. Data are shown as mean+SEM. %IA/g: percent of the injected activity per
 398 gram. Asterisks indicate significance compared to i.v. application. * $p<0.05$; ** $p<0.01$; *** $p<0.001$.

⁶⁸Ga-DOTATOC



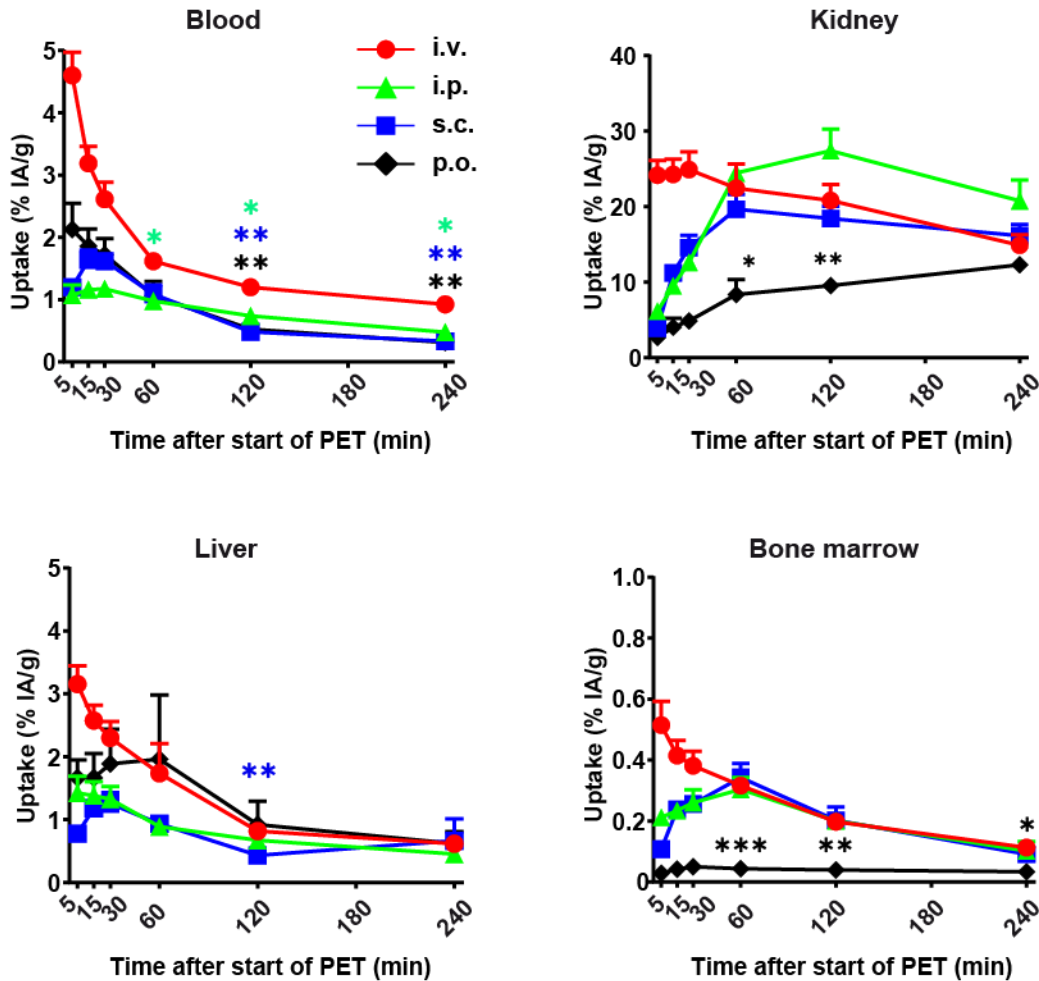
399

400

401 **Figure 2. In healthy mice, organ biodistribution at ≥ 1 h p.i following i.p. and s.c. radioligand**
402 **application is nearly equivalent to i.v. injection.** Healthy mice ($n=6$ /group) underwent PET
403 scans following i.v., i.p., s.c., and p.o. radioligand application, respectively, at minute 0-30 after
404 start of PET and after 1h, 2h and 4h with subsequent sacrifice of animals. Time-activity curves
405 illustrate *in vivo* PET biodistribution of ⁶⁸Ga-DOTATOC dynamics in VOIs at indicated times for
406 i.v., i.p., s.c., and p.o. application. Data are shown as mean+SEM. %IA/g: percent injected activity
407 per gram. Asterisks indicate significance compared to i.v. injection.* $p<0.05$.

408

⁶⁸Ga-PSMA



409

410

411

412

413

414

415

416

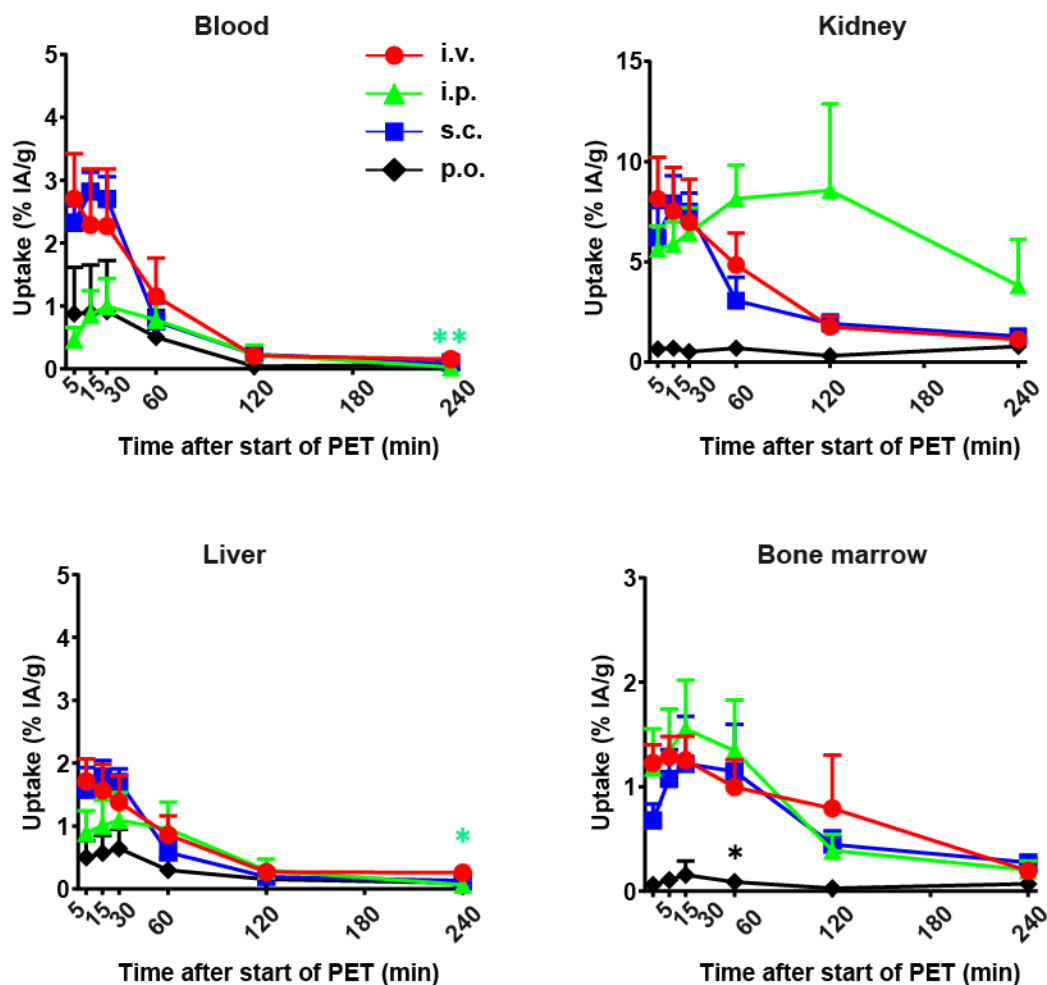
417

418

419

Figure 3. In healthy mice, organ biodistribution at ≥ 1 h p.i following i.p. and s.c. radioligand application is nearly equivalent to i.v. injection. Healthy mice ($n=6$ /group) underwent PET scans following i.v., i.p., s.c., and p.o. radioligand application, respectively, at minute 0-30 after start of PET and after 1h, 2h and 4h with subsequent sacrifice of animals. Time-activity curves illustrate *in vivo* PET biodistribution of ⁶⁸Ga-PSMA dynamics in VOIs at indicated times for i.v., i.p., s.c., and p.o. application. Data are shown as mean+SEM. %IA/g: percent injected activity per gram. Asterisks indicate significance compared to i.v. injection.* $p<0.05$; ** $p<0.01$; *** $p<0.001$.

⁶⁸Ga-FAPI



420

421

422

423

424

425

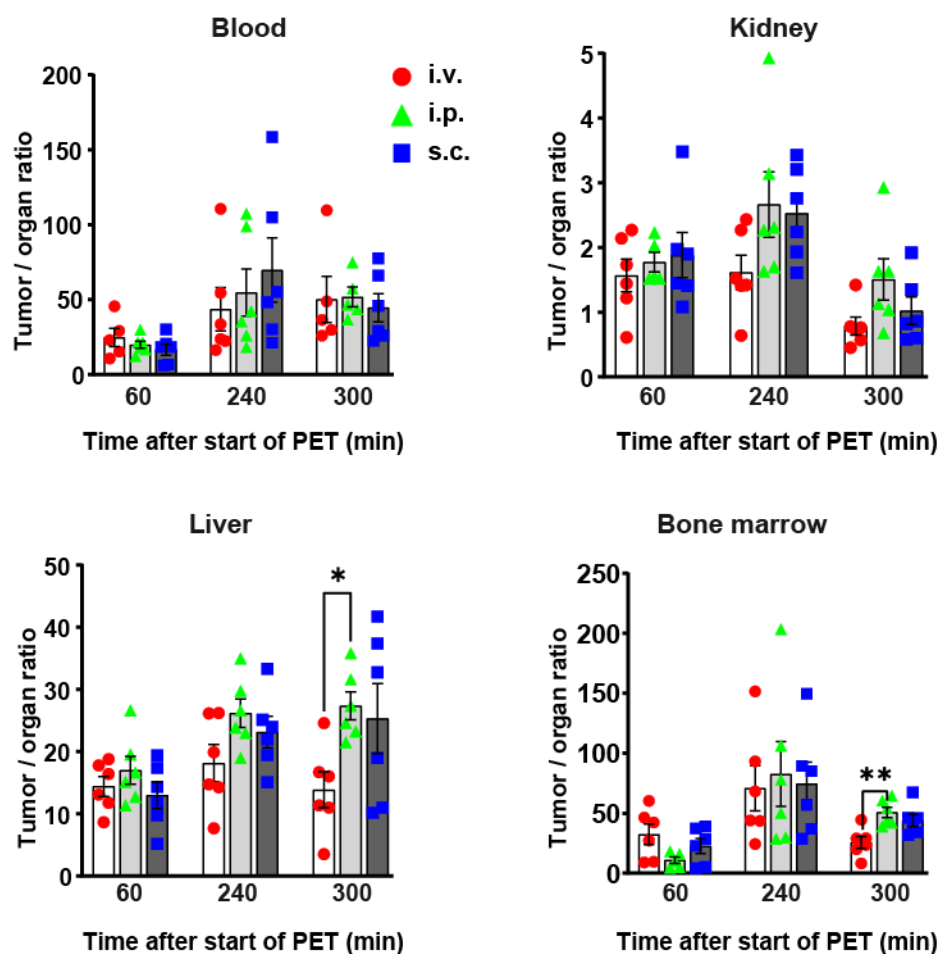
426

427

428

Figure 4. In healthy mice, organ biodistribution at ≥1h p. Healthy mice ($n=6$ /group) underwent PET scans following i.v., i.p., s.c., and p.o. radioligand application, respectively, at minute 0-30 after start of PET and after 1h, 2h and 4h with subsequent sacrifice of animals. Time-activity curves illustrate *in vivo* PET biodistribution of ⁶⁸Ga-FAPI dynamics in VOIs at indicated times for i.v., i.p., s.c., and p.o. application. Data are shown as mean+SEM. %IA/g: percent injected activity per gram. Asterisks indicate significance compared to i.v. injection. * $p<0.05$; ** $p<0.01$.

⁶⁸Ga-DOTATOC



429

430

431

432

433

434

435

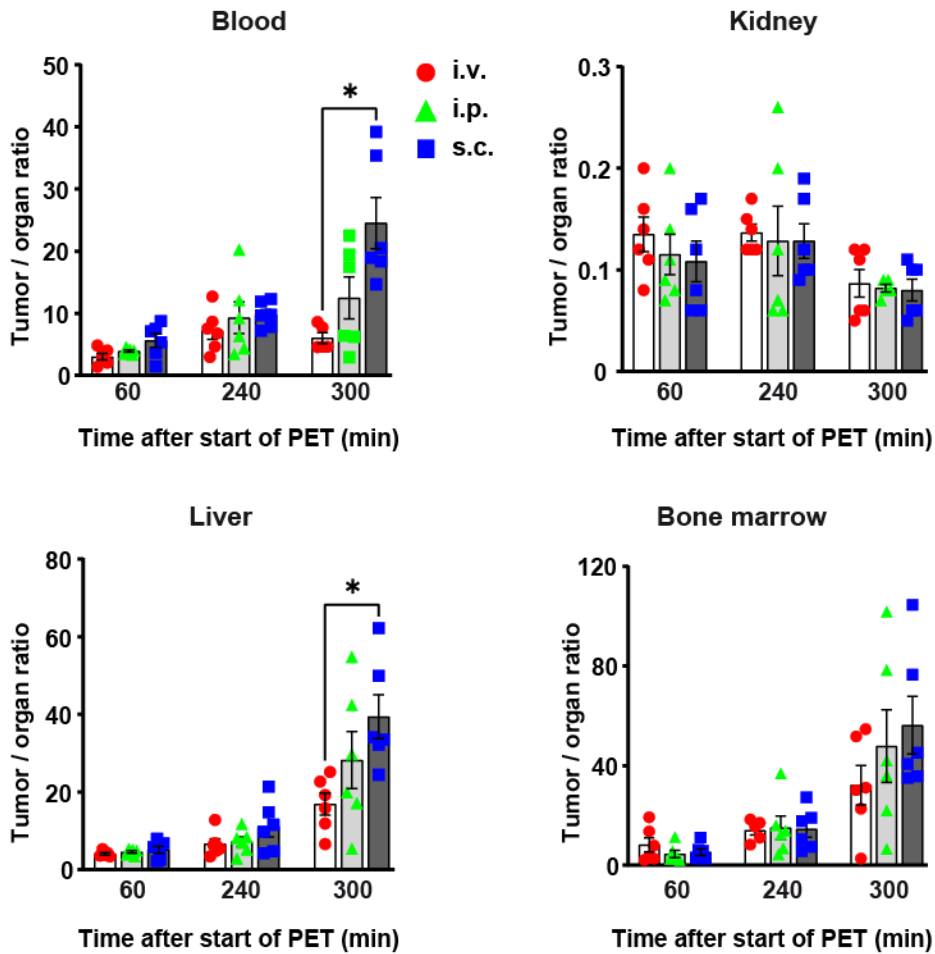
436

437

438

Figure 5. I.p. and s.c. radioligand application increase tumor-to-liver uptake compared to i.v. injection. Mice with subcutaneous RM1-SSTR tumors ($n=6$ /group) with i.v., i.p. and s.c. application of ⁶⁸Ga-DOTATOC and PET scans after 1h and 4h, followed by sacrifice (5h) and subsequent assessment of radioactivity in organs and tumors by gamma counter. Plots show tumor-to-organ ratios after i.v., i.p. and s.c. of ⁶⁸Ga-DOTATOC. Each dot represents a mouse. Data are shown as mean±SEM. Asterisks indicate significance compared to i.v. injection. *p<0.05; **p<0.01.

⁶⁸Ga-PSMA

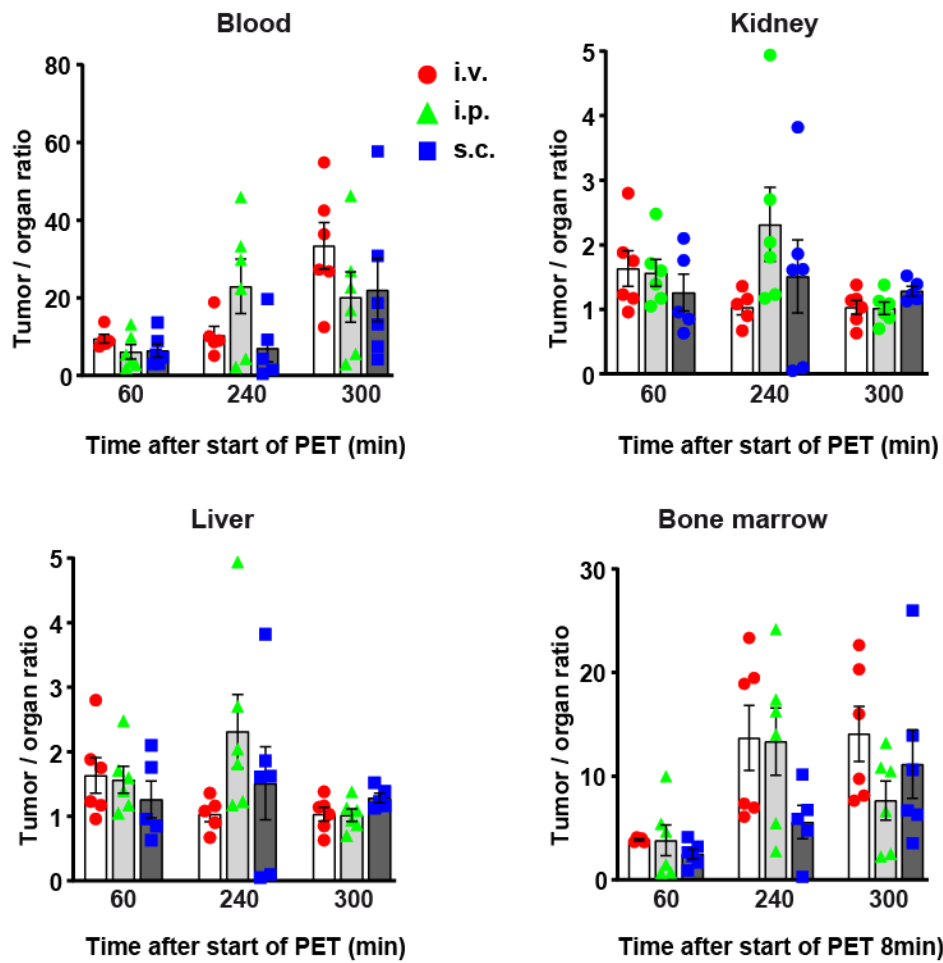


439

440

441 **Figure 6. I.p. and s.c. radioligand application increase tumor-to-liver uptake compared to**
442 **i.v. injection.** Mice with subcutaneous RM1-PSMA tumors ($n=6$ /group) with i.v., i.p. and s.c.
443 application of ⁶⁸Ga-PSMA and PET scans after 1h and 4h, followed by sacrifice (5h) and
444 subsequent assessment of radioactivity in organs and tumors by gamma counter. Plots show
445 tumor-to-organ ratios after i.v., i.p. and s.c. of ⁶⁸Ga-DOTATOC. Each dot represents a mouse.
446 Data are shown as mean±SEM. Asterisks indicate significance compared to i.v. injection. * $p<0.05$.

⁶⁸Ga-FAPI



447

448

449

450

451

452

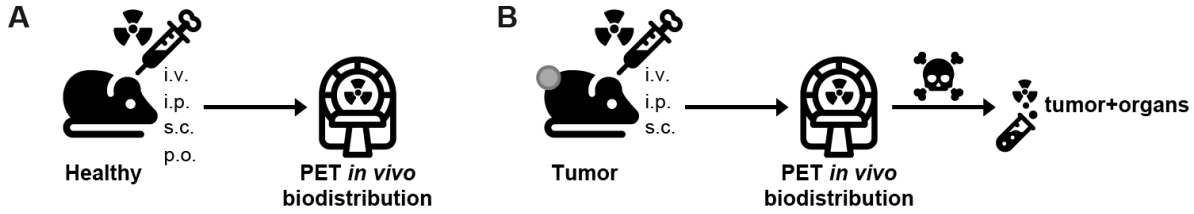
453

454

Figure 7. I.p. and s.c. radioligand application increase tumor-to-liver uptake compared to i.v. injection. Mice with subcutaneous HT-1080 tumors ($n=6/\text{group}$) with i.v., i.p. and s.c. application of ⁶⁸Ga-DOTATOC and PET scans after 1h and 4h, followed by sacrifice (5h) and subsequent assessment of radioactivity in organs and tumors by gamma counter. Plots show tumor-to-organ ratios after i.v., i.p. and s.c. of ⁶⁸Ga-DOTATOC. Each dot represents a mouse. Data are shown as mean \pm SEM.

455
456

GRAPHICAL ABSTRACT

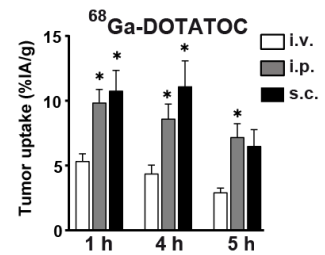
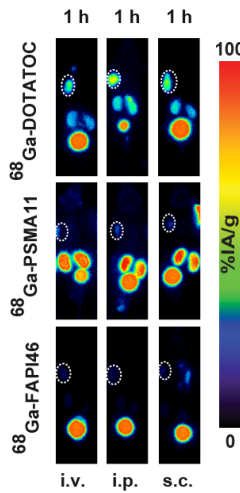
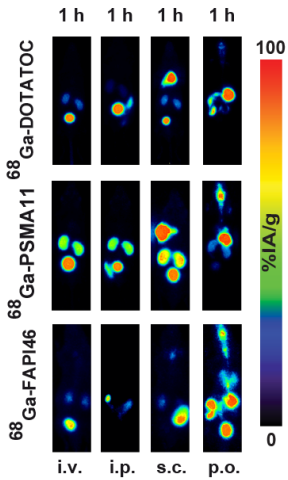


Comparable biodistribution after i.p. / s.c. versus i.v.



Comparable biodistribution after i.p. / s.c. versus i.v.

Increased tumor uptake after i.p. / s.c. versus i.v. ↑



457
458

1 Supplement

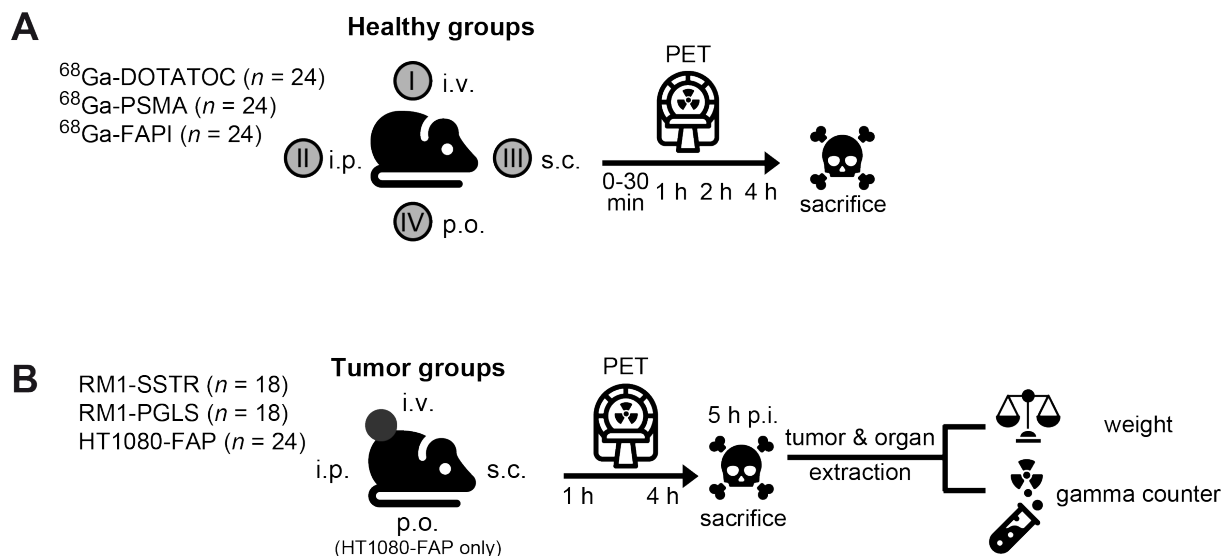
2 Supplemental Tables

3 **Supplemental Table 1. i.v., i.p., and s.c. injection led to near equivalent organ**
4 **biodistribution of radioligands in healthy mice.** Healthy mice were injected with
5 ^{68}Ga -DOTATOC, ^{68}Ga -PSMA11, or ^{68}Ga -FAPI46, respectively. Absolute organ uptake is given as
6 %IA/g at 1h and 4h p.i. (*in vivo* PET), and 5h p.i. (*ex vivo* gamma counter). Data represent mean
7 %IA/g \pm SEM of $n=6$ mice/group. * $p<0.05$; ** $p<0.01$.

^{68}Ga -DOTATOC					
	i.v.	i.p.	s.c.	p-value i.v. vs. i.p.	p-value i.v. vs. s.c.
blood 1h	1.3 \pm 0.3	1.0 \pm 0.1	1.1 \pm 0.1	0.7589	0.8431
blood 4h	0.3 \pm 0.1	0.2 \pm 0.02	0.2 \pm 0.04	0.5639	0.8229
kidneys 1h	6.0 \pm 1.0	6.2 \pm 0.4	5.6 \pm 0.5	0.9965	0.9837
kidneys 4h	3.9 \pm 0.7	4.3 \pm 0.2	5.9 \pm 0.5	0.9393	0.1658
^{68}Ga -PSMA11					
	i.v.	i.p.	s.c.	p-value i.v. vs. i.p.	p-value i.v. vs. s.c.
blood 1h	1.6 \pm 0.1	1.0 \pm 0.1	1.1 \pm 0.1	$p=0.0226^*$	$p=0.0880^*$
blood 4h	0.9 \pm 0.1	0.5 \pm 0.1	0.3 \pm 0.04	$p=0.0394^*$	$p=0.0065^{**}$
kidneys 1h	22.4 \pm 3.2	24.4 \pm 0.9	19.7 \pm 2.0	$p=0.9279$	$p=0.8773$
kidneys 4h	14.9 \pm 1.4	20.8 \pm 2.8	16.1 \pm 1.5	$p=0.3040$	$p=0.9251$
^{68}Ga -FAPI46					
	i.v.	i.p.	s.c.	p-value i.v. vs. i.p.	p-value i.v. vs. s.c.
blood 1h	1.2 \pm 0.6	0.8 \pm 0.4	0.8 \pm 0.3	$p=0.9505$	$p=0.9345$
blood 4h	0.2 \pm 0.02	0.02 \pm 0.01	0.1 \pm 0.03	$p=0.0036^{**}$	$p=0.5326$
kidneys 1h	4.9 \pm 1.6	8.7 \pm 1.7	3.1 \pm 1.2	$p=0.5065$	$p=0.8014$
kidneys 4h	1.1 \pm 0.2	3.8 \pm 2.3	1.3 \pm 0.2	$p=0.6694$	$p=0.9513$

9 Supplemental Figures

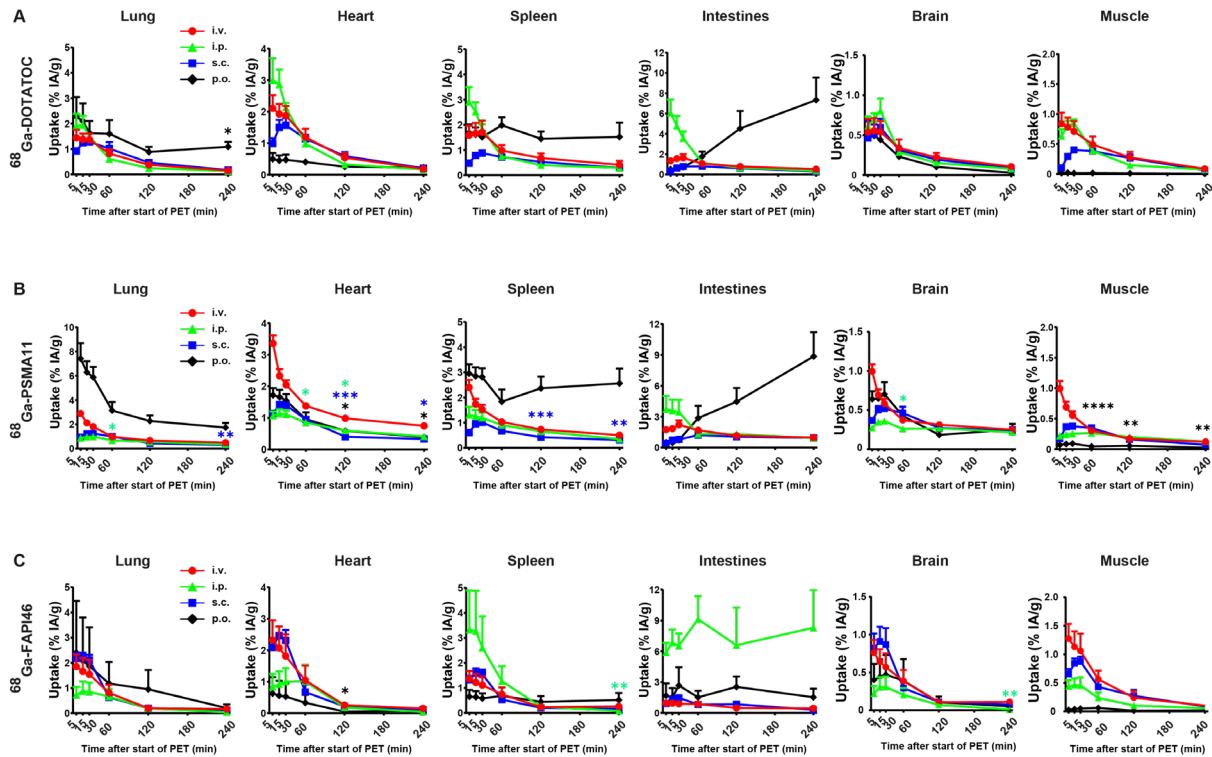
10



11

12 **Supplemental Figure 1. Experimental design.** (A) Healthy mice ($n=6$ /group) underwent PET
13 scans following i.v., i.p., s.c., and p.o. radioligand application, respectively, at minute 0-30 after
14 start of PET and after 1h, 2h and 4h with subsequent sacrifice of animals. (B) Mice with
15 subcutaneous RM1-SSTR, RM1-PSMA, or HT1080-FAP tumors ($n=6$ /group) with i.v., i.p. and s.c.
16 application of ^{68}Ga -DOTATOC, ^{68}Ga -PSMA11, or (C) ^{68}Ga -FAPI46, respectively underwent PET
17 scans after 1h and 4h, followed by sacrifice (5h) and subsequent assessment of radioactivity in
18 organs and tumors by gamma counter.

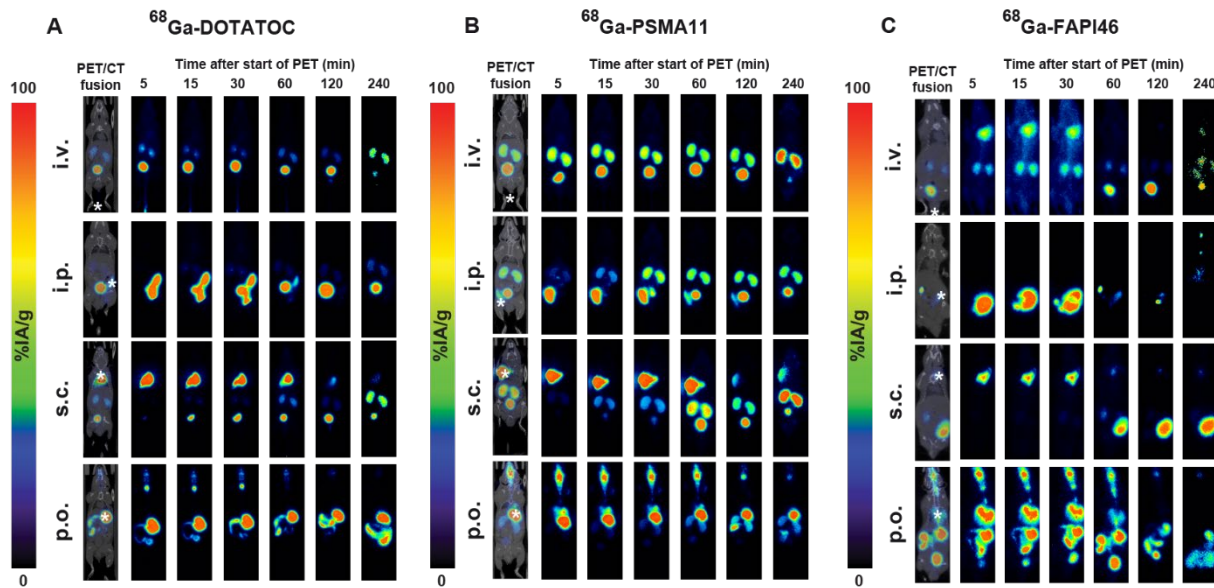
19



20
 21 **Supplemental Figure 2. Near equivalent radioligand organ biodistribution for i.p. and s.c.**
 22 **compared to i.v. injection in healthy mice.** *In vivo* PET biodistribution of ^{68}Ga -ligands in healthy
 23 mice ($n=6/\text{group}$). PET scans with (A) ^{68}Ga -DOTATOC, (B) ^{68}Ga -PSMA11, and (C) ^{68}Ga -FAPI46.
 24 Time-activity curves illustrate radioligand dynamics in selected organ VOIs at indicated time points
 25 for i.v., i.p., s.c., and p.o. application. Data are shown as mean+SEM. %IA/g: percent of the
 26 injected activity per gram. Asterisks indicate significance compared to i.v. application route.
 27 * $p<0.05$; ** $p<0.01$; *** $p<0.001$; **** $p<0.0001$.

28

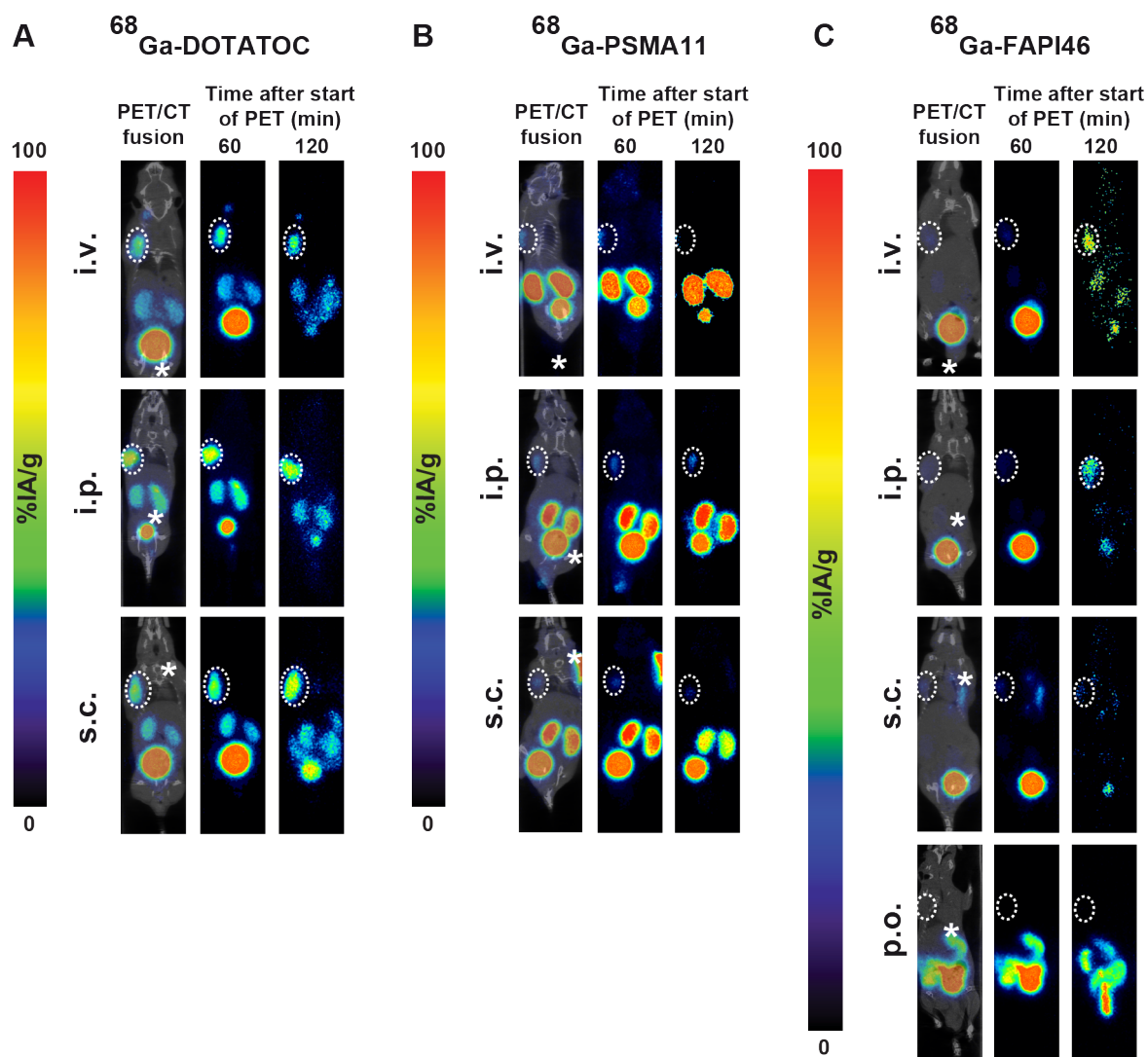
29



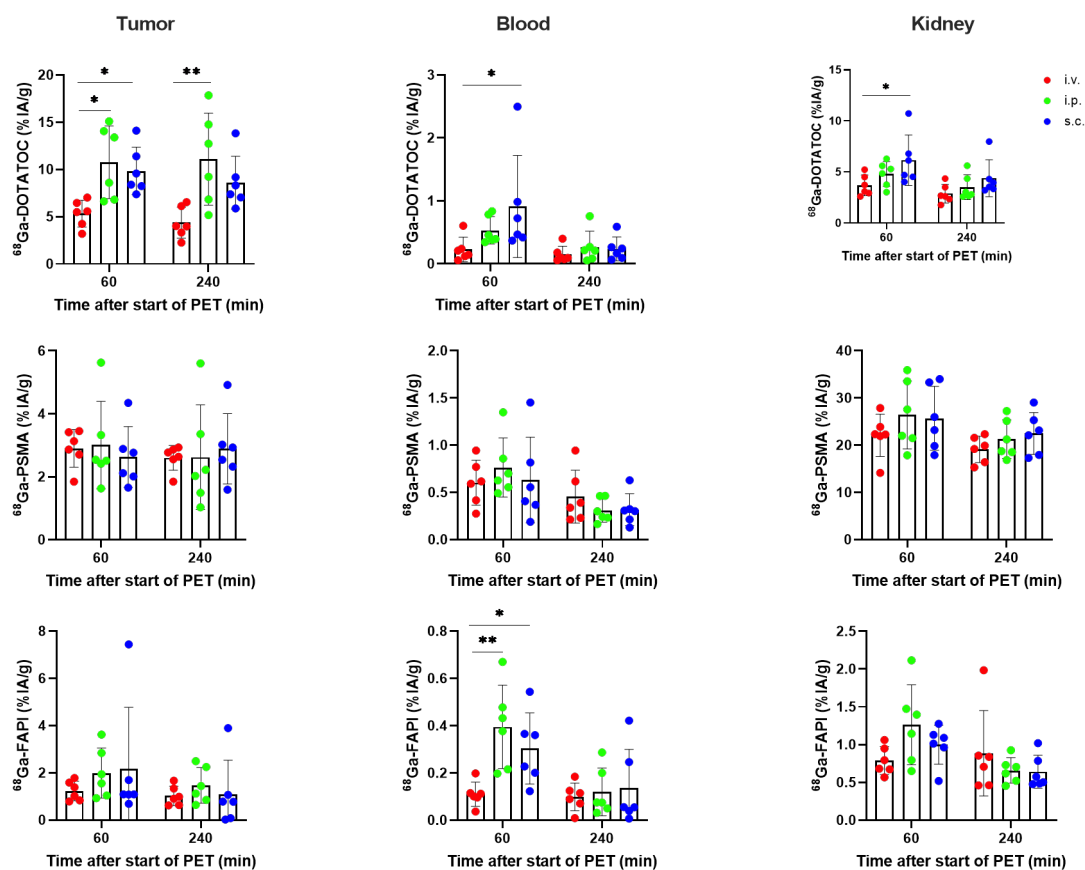
30
31 **Supplemental Figure 3. PET biodistribution of ^{68}Ga -ligands in healthy mice.** Whole body
32 maximum intensity projections of one representative mouse out of $n=6$ /group for each application
33 route after injection of ^{68}Ga -labelled ligands. (A) ^{68}Ga -DOTATOC, (B) ^{68}Ga -PSMA11, and
34 (C) ^{68}Ga -FAPI46 after i.v., i.p., s.c., and p.o. application in healthy mice. Asterisks indicate the
35 injection site.

36

37

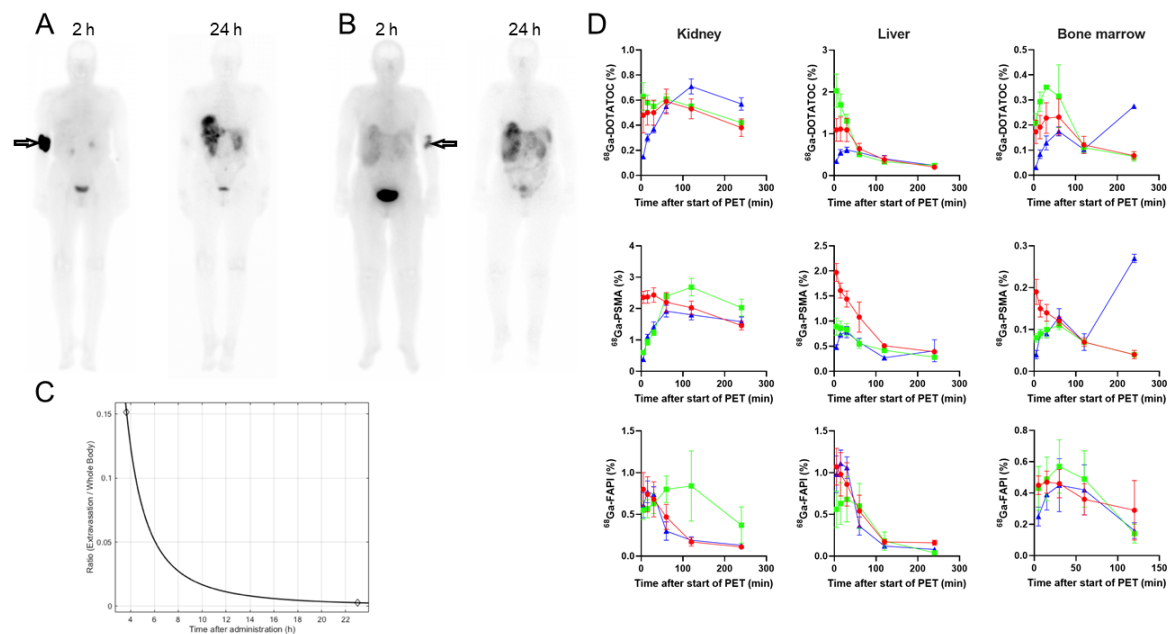


39
40 **Supplemental Figure 4. PET biodistribution of ^{68}Ga -ligands in tumor-bearing mice.** Whole
41 body maximum intensity projections of one representative mouse out of $n=6$ /group for each
42 application route 1h and 4h after injection of ^{68}Ga -labelled ligands. (A) ^{68}Ga -DOTATOC, (B)
43 ^{68}Ga -PSMA11, and (C) ^{68}Ga -FAPI46 via i.v., i.p., and s.c. application in RM1-SSTR-, RM1-PSMA-
44 , or HT1080-FAP-tumor-bearing mice with additional p.o. application, respectively. Asterisks
45 indicate the injection site; dashed circles indicate subcutaneous tumor in the right shoulder region.



48
 49 **Supplemental Figure 5. PET biodistribution of ^{68}Ga -ligands in tumor-bearing mice. *In vivo***
 50 PET uptake of ^{68}Ga -ligands in tumor-bearing mice ($n=6/\text{group}$). after ^{68}Ga -DOTATOC, ^{68}Ga -
 51 PSMA11, and ^{68}Ga -FAPI46. Bars illustrate radioligand uptake in selected organ VOIs at indicated
 52 time points for i.v., i.p., and s.c. application. Data are shown as mean \pm SD. %IA/g: percent of the
 53 injected activity per gram. Asterisks indicate significance compared to i.v. application route.
 54 * $p < 0.05$; ** $p < 0.01$.

56



57

58 **Supplemental Figure 6.** Anterior whole-body planar images of ^{177}Lu -DOTATOC distribution 2h
59 and 24h after paravenous infusion (arrow) of the radioligand in two patients (A and B). Radioligand
60 absorption in patient A occurs with a half-life of 3.3 hours (C). Extrapolation from mice to humans
61 suggests comparable biodistribution of ^{68}Ga -radioligands in healthy organs (D). Data are shown
62 as mean \pm SEM.